



CHORUS

This is the accepted manuscript made available via CHORUS. The article has been published as:

Enhanced pairing in the checkerboard Hubbard ladder

George Karakonstantakis, Erez Berg, Steven R. White, and Steven A. Kivelson

Phys. Rev. B **83**, 054508 — Published 22 February 2011

DOI: [10.1103/PhysRevB.83.054508](https://doi.org/10.1103/PhysRevB.83.054508)

Enhanced Pairing in the “Checkerboard” Hubbard LadderGeorge Karakonstantakis,¹ Erez Berg,² Steven R. White,³ and Steven A. Kivelson¹¹*Department of Physics, Stanford University, Stanford, CA 94305, USA*²*Department of Physics, Harvard University, Cambridge, MA 02138, USA*³*Department of Physics and Astronomy, University of California, Irvine, CA 92717, USA*

We study signatures of superconductivity in a 2-leg “checkerboard” Hubbard ladder model, defined as an one-dimensional (period 2) array of square plaquettes with an intra-plaquette hopping t and inter-plaquette hopping t' , using the density matrix renormalization group method. The highest pairing scale (characterized by the spin gap or the pair binding energy, extrapolated to the thermodynamic limit) is found for doping levels close to half filling, $U \approx 6t$ and $t'/t \approx 0.6$. Other forms of modulated hopping parameters, with periods of either 1 or 3 lattice constants, are also found to enhance pairing relative to the uniform two-leg ladder, although to a lesser degree. A calculation of the phase stiffness of the ladder reveals that in the regime with the strongest pairing, the energy scale associated with phase ordering is comparable to the pairing scale.

REVIEW COPY
NOT FOR DISTRIBUTION

II. THE MODEL

We consider the repulsive U Hubbard model defined on a (spatially modulated) two-leg ladder

$$\begin{aligned} \mathcal{H} = & - \sum_{j,\lambda,\sigma} (t_{j,j+1} c_{j,\lambda,\sigma}^\dagger c_{j+1,\lambda,\sigma} + h.c.) \\ & - t \sum_{j,\sigma} (c_{j,1,\sigma}^\dagger c_{j,2,\sigma} + h.c.) + U \sum_{j,\lambda} n_{j,\lambda,\uparrow} n_{j,\lambda,\downarrow} \end{aligned} \quad (1)$$

Here $c_{j,\lambda,\sigma}^\dagger$ creates an electron on rung $j = 1, \dots, L-1$ of chain $\lambda = 1, 2$ with spin polarization $\sigma = \pm$, L is the length of the ladder, $U > 0$ is the repulsion between two electrons on the same site, the density operator is $n_{j,\lambda,\sigma} = c_{j,\lambda,\sigma}^\dagger c_{j,\lambda,\sigma}$, and $n = (2L)^{-1} \sum_{j,\lambda,\sigma} \langle n_{j,\lambda,\sigma} \rangle$ is the mean number of electrons per site. The much studied homogeneous Hubbard ladder corresponds to the case $t_{j,j+1} = t'$ for all j , although it is worth noting that for $t' \ll t$, this model can also be viewed as a coupled array of Hubbard-dimers. The “dimer ladder” is shown in Fig. 1a. The “checkerboard ladder” in Fig. 1b has $t_{2j,2j+1} = t$ and $t_{2j+1,2j+2} = t' < t$. The “period three” ladder in Fig. 1c has $t_{3j,3j+1} = t_{3j+1,3j+2} = t$ and $t_{3j+2,3j+3} = t' < t$.

The thermodynamic limit is accessed by computing quantities for various lengths, and then using finite size scaling analysis to extrapolate to $1/L \rightarrow 0$.

III. EFFECTIVE FIELD-THEORY

The uniform two-leg Hubbard ladder with $n \neq 1$ but still not too far from $n = 1$, is well known, on the basis of weak coupling RG¹¹, bosonization¹², and DMRG³ approaches, to be in a Luther-Emery phase characterized at low energies by a spin-gap, ΔE_s (defined in Eq. 4, below) and a single, gapless acoustic “charge” mode which propagates with speed v_c , and whose long-range (power-law) correlations are determined by a single Luttinger parameter, K_c . The Luther-Emery liquid can be thought of as a 1D version of a superconducting state in the sense that it has a non-vanishing superfluid stiffness (see Eq. 6, below), and, for $K_c > 1/2$ and $T \ll \Delta E_s$, it has a divergent superconducting susceptibility,

$$\chi \sim \chi_0 \left(\frac{v_c}{aT} \right)^{(2-1/K_c)}, \quad (2)$$

where v_c is the charge velocity and a is a lattice constant. In the single chain realization of a Luther-Emery liquid,

$$\chi_0 = \left(\frac{a}{v_c} \right) \left(\frac{a \Delta E_s}{v_s} \right) = \left(\frac{a}{v_c} \right) \left(\frac{a}{\xi_s} \right), \quad (3)$$

where $\xi_s = v_s/\Delta E_s$ is the spin-correlation length and v_s is the spin-velocity. For a multicomponent system, the corresponding expression for χ_0 is somewhat more complicated, as there may be multiple scales (*e.g.* multiple spin-gaps) associated with the gapped modes. However, χ_0 remains a monotonic, approximately linearly increasing function of ΔE_s .

Perhaps not surprisingly, we will see that the inhomogeneous Hubbard ladders we have studied are also Luther-Emery liquids with $K_c > 1/2$. Thus, in addressing the “mechanism of superconductivity,” the primary purpose of our DMRG calculations is to determine the dependence of v_c , K_c , ΔE_s and ξ_s on microscopic parameters.

The pair binding energy ΔE_p corresponds to creating two spatially-separated spin-1/2 quasiparticles. Since the spins for these quasiparticles can either add to $S = 0$ or 1, we must have $\Delta E_s \leq \Delta E_p$. If the residual interactions between quasiparticles are repulsive, we expect $\Delta E_s = \Delta E_p$. Conversely, if the interactions between quasiparticles are attractive, a neutral spin-1 “exciton” is formed, which has lower energy than two far-separated quasi-particles, and hence $\Delta E_s < \Delta E_p$. The latter behavior has been found previously in DMRG calculations on the uniform $t - J$ ladder¹³.

IV. ENERGY SCALES

The spin-gap, ΔE_s , is the difference between the ground-state energies of the system with spin $S = 1$ and $S = 0$:

$$\Delta E_s \equiv \mathcal{E}_0(S = 1, 2N) - \mathcal{E}_0(S = 0, 2N), \quad (4)$$

where $\mathcal{E}_0(S, N)$ is the spin S ground-state energy of the N electron system.

Similarly, the pair-binding energy, ΔE_p , is defined as

$$\Delta E_p = 2\mathcal{E}_0\left(\frac{1}{2}, 2N + 1\right) - \mathcal{E}_0(0, 2N) - \mathcal{E}_0(0, 2N + 2). \quad (5)$$

Were we computing these quantities in a BCS superconductor, then in the thermodynamic limit, both these energies would be equal to twice the minimum gap Δ_{\min}

$$\lim_{L \rightarrow \infty} \Delta E_s = \lim_{L \rightarrow \infty} \Delta E_p = 2\Delta_{\min}.$$

What we have in mind here is a system with a strongly k dependent superconducting gap. In 2D, then, the value of the gap would depend on the position on the Fermi surface. For a ladder with a finite number of legs, there are a discrete set of transverse values of k , so even in the thermodynamic limit, only certain discrete points on what would, in 2D, be a full Fermi surface are crossed. In this case, in the thermodynamic limit, the gap we would obtain will be the gap that occurs at the point on the 2D Fermi surface where the gap happens to be smallest. For an s-wave superconductor, this is a reasonable measure of the gap in 2D. For a d-wave SC, the precise value depends on how close the closest Fermi surface crossing is to the nodal point. Thus, it is intuitively reasonable to associate these energy scales with a mean-field estimate of the superconducting critical temperature, $T_c^{MF} \sim \Delta E_s/4$. Of course, since the ladder is a 1D system, the actual $T_c = 0$.

While it may be reasonable to interpret ΔE_s and/or ΔE_p as measures of a pairing scale in the problem, in order to address the growth of superconducting correlations it is ultimately necessary to consider the helicity modulus, which governs the energetics of superconducting phase fluctuations:

$$\rho_c = \frac{v_c K_c}{2\pi} \equiv \lim_{L \rightarrow \infty} \left[L \frac{\partial^2 \mathcal{E}_0}{\partial \phi^2} \Big|_{\phi=0} \right] \quad (6)$$

where, in this case, the ground-state energy is computed in the presence of pair-fields applied to the two ends of the system with a relative phase twist ϕ .

In 2D, the relative importance of phase and pair-breaking fluctuations can be assessed¹⁴ by considering the ratio of the phase stiffness (which has units of energy) to the pairing gap. However, in 1D, ρ_c has units of a velocity, so defining an energy scale, ΔE_θ , characteristic of the phase fluctuations requires introducing a length scale in the problem. The important (longest) emergent length scale is ξ_s , in terms of which we define

$$\Delta E_\theta \equiv \pi \rho_c / \xi_s \equiv R \Delta E_s. \quad (7)$$

Here $R \equiv \Delta E_\theta / \Delta E_s$ is the dimensionless ratio of the phase ordering and pairing scales.

To appreciate the significance of this ratio, consider its value for the attractive Hubbard chain in various limits. The 1D version of a BCS limit, in which there is a single characteristic energy/temperature scale, $\Delta_s \sim \exp[-\pi v_s/a|U|]$, is realized in the limit $|U| \ll 1$ where, up to corrections of order U/t , $v_s = v_c$ and $K_c = 1$, so $R = v_c K_c / 2v_s = 1/2 + \mathcal{O}(U/t)$, *i.e.* both mesoscale phase coherence and pairing correlations onset at a temperature of the order of $T_{\text{pair}} \sim \Delta E_s/4$. Conversely, $R \rightarrow 0$ as $|U|/t \rightarrow \infty$; for large U , a spin pseudo-gap opens when $T \sim T_{\text{pair}} = |U|/2$, with a second crossover from a largely incoherent paired state to a coherent Luther-Emery liquid occurring at a temperature $T_\theta \sim \Delta E_\theta \propto t^2/|U|$, well below T_{pair} . A similar dichotomy exists in the two-leg repulsive U Hubbard ladder, where $R \rightarrow 0$ as the doped hole concentration, $x \rightarrow 0$, while $R \sim 1$ at larger values of x where the spin-gap is significantly suppressed relative to its value at $x = 0$. In the small x case, the doped holes can be thought of as a dilute gas of charge $2e$ bosons at temperatures small compared to T_{pair} , but the phase coherence scale is much smaller and vanishes as $x \rightarrow 0$.

With these examples in mind, we identify the case $R \sim 1$ with the 1D version of the ‘‘BCS-like limit’’ in which there is a single crossover temperature T_{pair} which separates the ‘‘normal’’ (multicomponent Luttinger liquid) high temperature regime from the low temperature regime in which substantial mesoscale superconducting order has developed. Conversely, if $R \ll 1$, two distinct crossover scales characterize the evolution from the normal state: a first, high temperature crossover, T_{pair} , characterized by the opening of a spin pseudo-gap, and a lower crossover temperature, $T_\theta \sim \Delta E_\theta/4$, which can be viewed as the scale at which the liquid of bosonic pairs begin to exhibit substantial local phase coherence.

The most direct and efficient way to compute ξ_s from DMRG is to apply a staggered Zeeman field to one end of the ladder, $j = 0$ (thus locally breaking spin-rotational symmetry) and then measure the decay of the magnetization as a function of distance down the ladder. In a spin-gapped phase, we expect

$$\begin{aligned} M(j) &= \sum_{\sigma} \sigma \langle [c_{j,1,\sigma}^\dagger c_{j,1,\sigma} - c_{j,2,\sigma}^\dagger c_{j,2,\sigma}] \rangle \\ &\sim \cos[Qj + \phi_0] \exp[-|j|a/\xi_s]. \end{aligned} \quad (8)$$

In the limit of an asymptotically small spin-gap, $Q = 2k_F$, but for larger gaps it may depend not only on n but on U/t as well. To be explicit, we therefore define the spin correlation length as

$$\xi_s = \frac{\sum_j |j M(j)|}{\sum_j |M(j)|}. \quad (9)$$

It turns out that Eq. 6 is relatively difficult to implement to obtain quantitatively reliable results for ρ_c using DMRG. However, it is possible¹⁵ to compute ρ_c by separately calculating v_c and v_c/K_c from quantities that are more straightforwardly computed using DMRG. From the bosonized field theory, we can identify the inverse compressibility of the ladder with the ratio $\frac{\pi v_c}{2K_c}$. In turn, in all circumstances relevant to the present calculation¹⁶, the compressibility is related to the energy to add or remove a singlet pair of electrons from the ladder:

$$\frac{1}{\kappa} = \lim_{L \rightarrow \infty} L \frac{\mathcal{E}_0(0, 2N+2) + \mathcal{E}_0(0, 2N-2) - 2\mathcal{E}_0(0, 2N)}{4}, \quad (10)$$

An independent measurement of v_c can be obtained by calculating also the energy of the first excited state, $\mathcal{E}_1(S, N)$ according to

$$v_c = \lim_{L \rightarrow \infty} \frac{L}{\pi} [\mathcal{E}_1(0, 2N) - \mathcal{E}_0(0, 2N)]. \quad (11)$$

We then compute the helicity modulus as

$$\rho_c = \frac{v_c^2 \kappa}{4}. \quad (12)$$

Note that this procedure also gives us

$$K_c = \frac{\pi}{2} \kappa v_c. \quad (13)$$

An alternative way to obtain K_c is by measuring the amplitude of the ‘‘Friedel-like’’ density oscillations which exhibit a power-law decay as a function of distance from the edge of the system. For long systems, the density near the center of a length L ladder takes the form¹⁵

$$\langle n_j \rangle \sim \frac{\cos[2\pi n(j - L/2)]}{L^{K_c/2}}. \quad (14)$$

Therefore, by measuring the amplitude of the density oscillations A_{CDW} vs. L and plotting $\log(A_{\text{CDW}})$ vs. $\log(L)$, K_c can be obtained. Whenever possible, we have calculated K_c using both Eq. 13 and Eq. 14, and found that the two values agree with each other to within about 10%.

V. DMRG RESULTS

We have computed ground state properties for ladder systems for various values of n , t'/t , and U/t using DMRG. We have kept up to $m = 2400$ states and extrapolated our results to zero truncation errors. As is well known,¹⁷ ground state energies (as well as one-point correlation functions¹⁸) can be extracted with great accuracy in this way. Results have been obtained for system sizes from 2×16 up to 2×64 , and then extrapolated to the thermodynamic limit ($1/L \rightarrow 0$) using a finite size scaling analysis. For an example of this procedure, see Appendix A. Since DMRG converges better for open boundary conditions, all the calculations were done using open boundary conditions in the long direction. From the extrapolated values, we have extracted ΔE_s , ξ_s , ΔE_p , ρ_c , and K_c , as described above.

In Fig.2, we show ΔE_s for fixed $U/t = 8$ [?] as a function of t'/t for $n = 0.9375$, 0.875 , and 0.75 . Note that the value of ΔE_s rises from its value for the uniform ladder as t'/t is reduced below $t'/t = 1$, reaches a maximum value at an intermediate value of t'/t , and then drops to zero as $t'/t \rightarrow 0$. For instance, for $n = 0.875$, the maximum value $\Delta E_s \approx 0.12t$, which occurs for $t'/t = 0.6$, is approximately 4 times larger than its value in the uniform ladder. More broadly, we have studied the spin gap as a function of both U/t and t'/t ; the results for $n = 0.875$ are shown in Fig. 3. One can see that ΔE_s exhibits a broad maximum for U of order the band-width ($U \sim 4 - 8t$) and intermediate inhomogeneity, $t'/t \sim 0.5$. This figure looks qualitatively similar to the analogous result for the two dimensional checkerboard Hubbard model obtained previously by exact diagonalization of a 16 site system in Ref. 5; however, in contrast to that study, the present results are obtained in the thermodynamic limit.

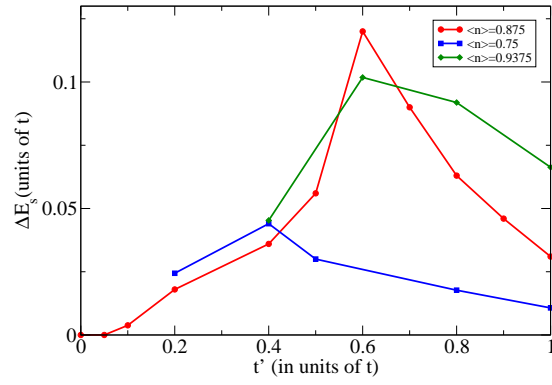


FIG. 2. The spin-gap, ΔE_s , of the checkerboard-Hubbard ladder as a function of t'/t for $n = 0.9375$, 0.875 , and 0.75 at fixed $U = 8t$, extrapolated to the thermodynamic limit ($L \rightarrow \infty$).

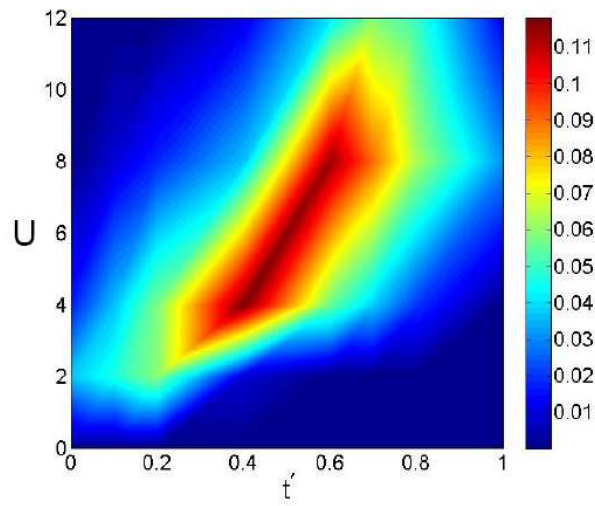


FIG. 3. $\Delta E_s(L \rightarrow \infty)$ of the checkerboard Hubbard ladder for $n = 0.875$ as a function of U and t' , fixing $t = 1$.

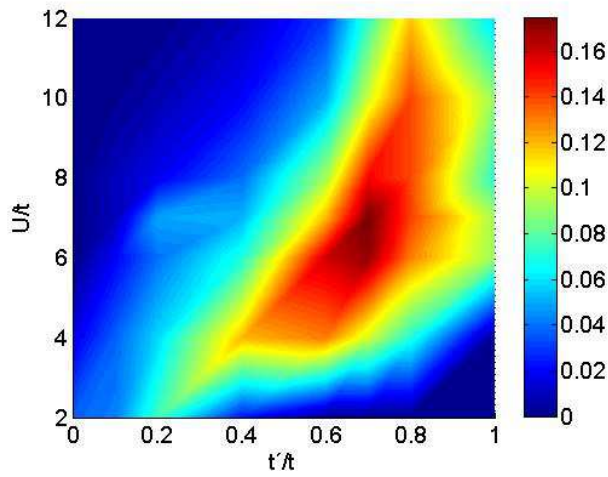


FIG. 4. The pair binding energy, ΔE_p , of the checkerboard Hubbard ladder for $n = 0.875$ (in the thermodynamic limit) as a function of U and t' , fixing $t=1$.

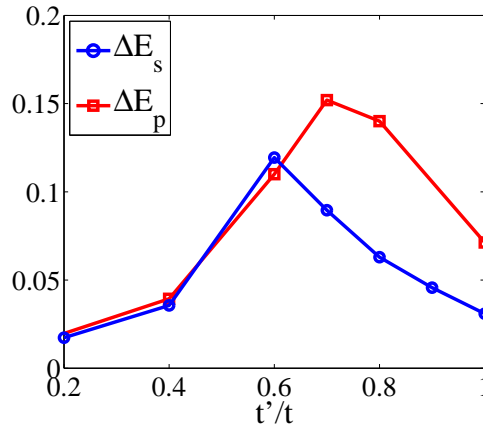


FIG. 5. $\Delta E_s(L \rightarrow \infty)$ and $\Delta E_p(L \rightarrow \infty)$ for the checkerboard ladder with fixed $n = 0.875$ and $U/t = 8$, as a function t'/t .

The dependence of ΔE_p on U/t and t'/t is generally similar to that of ΔE_s , as can be seen by comparing the contour plots of these two quantities for $n = 0.875$ which are shown in Fig. 4 and Fig. 3, respectively. However, there are interesting differences, as can be seen in Fig. 5, where the two quantities are plotted as a function of t'/t for fixed $U/t = 8$ and $n = 0.875$. Note that for $t'/t > 0.6$, $\Delta E_p > \Delta E_s$. This is, presumably, indicative of the existence of a spin 1 excitonic bound-state for $t'/t > 0.6$. A similar result was found in the uniform two-leg $t - J$ model ladders^{13,19}.

In order to calculate $R = \Delta E_\theta / \Delta E_s$, we must compute ρ_c and ξ_s . To obtain ξ_s , we apply a relatively strong staggered Zeeman field of magnitude t to the end sites of the ladder and measure the decay of the staggered magnetization, $M(j)$ as in Eq. 8. In all cases, we have found that $M(j)$ decays rapidly on scales short compared to the length of our longest ladders, so ξ_s can be extracted from the calculations accurately. Representative results for $M(j)$ are shown in the inset of Fig. 6. ξ_s as a function of t'/t is shown in Fig. 6, for fixed $n = 0.875$ and $U/t = 8$. Note that for $t'/t < 1/2$, the spin-correlation length is roughly $3a$, which is of the order of one unit cell of the checkerboard ladder.

Next, we calculate both ρ_c and K_c following the procedure described above [Eqs. 10–14]. The value of K_c is shown in Fig. 7 for $n = 0.75, 0.875$, and 0.9375 , fixing $U/t = 8$, as a function of t'/t . In contrast to the results for ΔE_s (and somewhat to our surprise), for $n = 0.875$, K_c is a weakly varying function of t'/t (and, as it turns out, U/t as well). To a good approximation, for a wide range of values, we can simply take $K_c \approx 1$, independent of t'/t and U/t . Note that this implies that the superconducting susceptibility diverges as $T \rightarrow 0$, so that it is reasonable to think of the ladder as a fluctuating superconductor. (Of course, there is also a divergent charge-density wave susceptibility, $\chi_{\text{CDW}} \sim T^{-(2-K_c)}$, so there is some unavoidable ambiguity with this simple intuitive picture.) As n is increased to 0.9375 , K_c increases, consistent with the expectation that $K_c \rightarrow 2$ as $n \rightarrow 1$.²⁰

TABLE I. Values of the ratio R defined in Eq. 7 for $n = 0.875$ and $U = 8t$.

t'/t	0.2	0.4	0.6	0.7	0.8	1.0
R	3.38	3.06	0.96	1.01	0.99	0.98

From the measured values of ξ_s , κ , and K_c , the energy scale characteristic of phase-ordering can be extracted. Table I shows the ratio R from Eq. 7. Note that for $t'/t > 0.5$, $R \approx 1$. Thus, at least crudely, this regime can be thought of as a “BCS like” regime, in which there is a single energy scale, set by ΔE_s , which characterizes the growth of superconducting correlations. Depending on precisely what criterion one chooses to quantify the crossover scale, phase fluctuations will produce a quantitative difference in the magnitude of the specified scale, but not large qualitative effects. Therefore, it is reasonable to assert that the values of the parameters which lead to the largest values of ΔE_s and/or ΔE_p are the “optimal values for superconductivity.”

For $t' < 0.5t$, we obtain $R \sim 3$, i.e. $\Delta E_\theta > \Delta E_s$, suggesting that this regime cannot be thought of in terms of either a naive weak or strong coupling picture. Remarkably, the transition from $R \sim 1$ to $R > 3$ occurs quite sharply around $t' = 0.5$, close to the point where the spin gap is optimal.

It is interesting to note that for $n = 0.75$, $t'/t = 0.4$ we find a sharp decrease of K_c and ρ_c . The value of K_c at this point is smaller than the critical value of 1 at which a static charge-density wave should be stable¹⁵, indicating that this behavior of K_c and ρ_c may be due to a charge-density wave phase that exists for $n = 0.75$, $t' \lesssim 0.4t$.

We thus conclude that for the checkerboard Hubbard ladder, optimal superconductivity occurs for intermediate values of $U/t \sim 6$, intermediate inhomogeneity, $t'/t \sim 0.6 - 0.7$, and electron concentrations near (but not equal

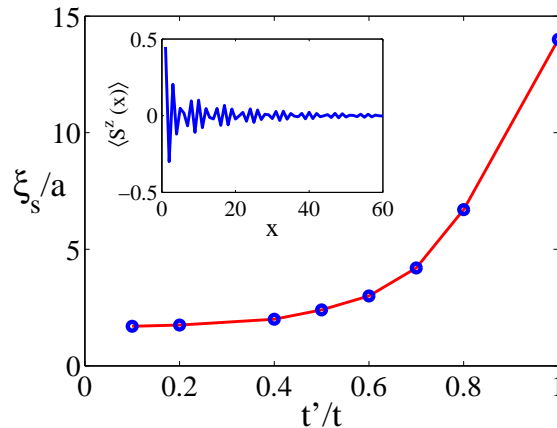


FIG. 6. The spin correlation length, ξ_s , for the checkerboard ladder with $U = 8t$ and $n = 0.875$ as a function of t'/t , calculated from Eq. 9. The inset shows the expectation value of the spin $\langle S^z \rangle$ for $U = 8t$, $n = 0.875$, and $t'/t = 1$, as a function of position. A staggered Zeeman field of strength t has been applied to the two sites at the left edge of the ladder.

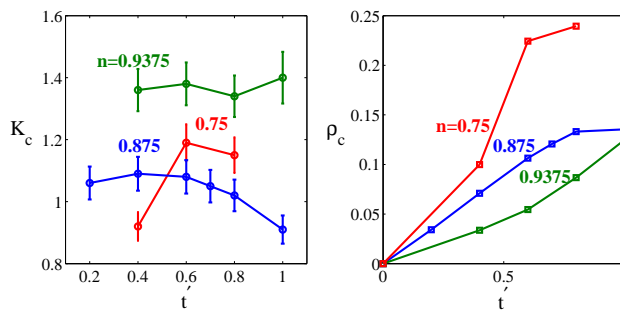


FIG. 7. Left: the Luttinger parameter K_c as a function of t'/t for $n = 0.75, 0.875$ and 0.9375 and $U = 8t$. The error bars were estimated by comparing between the values of K_c obtained from Eq. 13 and Eq. 14. Note that according to our definition of K_c , the non-interacting value is $K_c =$ function of t'/t .

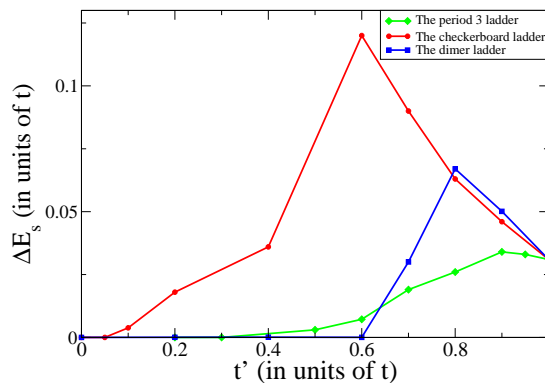


FIG. 8. $\Delta E_s(L \rightarrow \infty)$ for the three types of inhomogeneous ladders in Fig. 1 is shown at fixed $n = 0.875$ and $U/t = 8$ as a function of t'/t . The inhomogeneity induced by breaking up the ladders to period 1, 2 and 3 clusters increases the spin gap for $t'/t < 1$. The increase is most dramatic for the checkerboard ladder, in which the maximum spin gap is about 4 times larger than the spin gap for the uniform ($t' = 1$) system. For the period 1 (dimer) ladder, the enhancement is by a factor of 2, while for the period 3 ladder the spin gap is only slightly enhanced (by about 10%).

to) one electron per site. We can now ask if this result is special to the checkerboard pattern, or if it applies more generally to the situation in which there are multiple sites per unit cell. We thus have repeated (although not in as much detail) the same calculations for the dimer ladder (period 1) and the period 3 ladder. (See Fig. 1.)

In Fig. 8 we exhibit the dependence of the spin-gap of all three ladders for fixed $U = 8t$ and $n = 0.875$ as a function

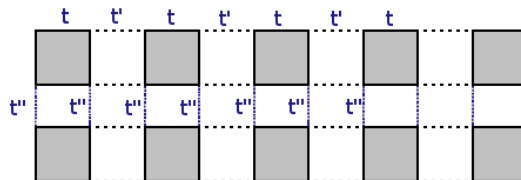


FIG. 9. A system of coupled checkerboard ladders, connected with by a single particle tunneling matrix element t''

of t'/t . In all the cases we see that there is an increase in the spin gap for some $t'/t < 1$.

The result was expected, qualitatively, in the dimer (period one) case from previous works^{3,4,21}, which found that the spin gap (as well as pairing correlations) is enhanced upon making t' smaller than t in the dimer (period 2) ladder. In the case of the period three ladders, there is a very weak increase of the spin gap, which occurs at $t'/t \sim 0.9$.

In Refs. 4, it was argued that the enhancement of superconducting correlations in the dimer ladder is due to the increase in the density of states close to the “Van Hove” point, in which one of the two bands of the two-leg ladder becomes unoccupied. Beyond this point, there is only a single band crossing the Fermi level, and the system is likely to behave as a single-component Luttinger liquid. Therefore the superconducting signatures are rapidly suppressed. Consistently with this picture, in the dimer ladder, we find that the spin gap collapses to zero below $t'/t \lesssim 0.6$. In the period 2 (the checkerboard ladder) and period 3 cases, however, no such sudden suppression of the spin gap is observed as t'/t is reduced below the optimal point. This leads us to believe that the mechanism of the enhancement of the spin gap for $t' < t$ in the checkerboard and period 3 ladders is unlikely to be related to a proximity to a Van Hove point.

Note also that for all the inhomogeneous patterns in Fig. 8, the spin gap seems to reach zero at a critical $t'_c > 0$ (which is different for each pattern). In particular, for the “checkerboard” pattern, $t'_c \sim 0.05t$. It is likely that for $t' < t'_c$, the Luther-Emery phase gives way to a Luttinger liquid phase with one gapless charge mode and gapless spin mode (or more), although more work is needed to establish that.

Overall, among all the patterns we have reported, the optimal ladder for superconductivity is a checkerboard ladder with $U = 6t$, $t'/t = 0.6 - 0.8$, and $n = 0.875$, for which $\Delta E_s = 0.12t$, $\Delta E_p = 0.16t$.

VI. EXTENSION TO QUASI 1D

Above, we have argued that the superconducting tendency in the checkerboard-Hubbard ladder is optimized for an intermediate value of t'/t . However, since the superconducting T_c of that system (as in any one-dimensional system) is strictly zero, one can worry that this statement may depend on how one chooses to measure the strength of the superconducting correlations. We will now consider a system composed of an array of parallel checkerboard-Hubbard ladders coupled weakly in the direction transverse to the ladders, in which T_c can be estimated in a controlled way based on the solution of the single-ladder problem. We will show that T_c is maximal for $\frac{t'}{t} < 1$. Thus, in this system, T_c is indeed optimized when the electronic structure is non-uniform; *i.e.*, there is an “optimal degree of inhomogeneity” for superconductivity.

The quasi-1D system of coupled checkerboard Hubbard ladders is depicted in Fig. 9. The ladders are coupled by a single particle tunneling matrix element t'' . We fix the value of $t'' \ll t, t'$, and estimate $T_c(t'/t)$ from an inter-chain mean field theory, described in Appendix B. From the numerical results for the checkerboard-Hubbard ladder with $n = 0.875$ and $U = 8t$ we recall that $K_c\left(\frac{t'}{t}\right) \approx 1$ over the entire range $0 < t' \leq 1$ (see Fig. 7). We therefore fix $K_c = 1$, independent of t' . The resulting expression for T_c is

$$T_c \sim \frac{K(\sqrt{1-x^2})}{x} \Delta E_s \left(\frac{at''}{v_c}\right)^2. \quad (15)$$

Here, $x \equiv v_s/v_c$, and $K(x)$ is a complete elliptic integral of the first kind. Note that T_c depends on t'/t through v_s , v_c and ΔE_s . As t' decreases, both v_c and v_s decrease; their ratio, however, is found to be approximately constant as a function of t'/t down to about $t'/t = 0.5$. (v_s is obtained by using the estimate $\Delta E_s \xi_s$, where both ΔE_s and ξ_s are calculated from DMRG.) $\Delta E_s\left(\frac{t'}{t}\right)$, on the other hand, has a maximum for $\frac{t'}{t} < 1$. Therefore, as $\frac{t'}{t}$ is reduced from 1, $T_c(t')$ necessarily increases, and reaches a maximum for some $t'_{\max} < t$.

VII. DISCUSSION

The present study, along with a variety of other recent studies^{5,8,9,22}, provide strong support for a number of intuitively appealing ideas concerning the physics of the superconducting T_c in unconventional superconductors in which the pairing arises directly from the repulsive interactions between electrons: 1) The highest superconducting transition temperatures occur at intermediate interaction strength, when U is comparable to the band-width. (A corollary of this is that materials which are studied because of their high transition temperatures are also likely to exhibit more general signatures of lying in an intermediate coupling regime; here, theoretical results from both weak and strong coupling approaches must be extrapolated, at best, to the limits of their regimes of applicability.) 2) Certain mesoscale structures (“optimal inhomogeneity”¹) can lead to enhanced superconducting pairing, although clearly if the system is too strongly inhomogeneous, that always leads to a suppression of global phase coherence. 3) While short-range magnetic correlations, possibly of the sort envisioned in the putative RVB state of a quantum antiferromagnet or in certain theories of a spin-fluctuation exchange mechanism, may well be important for pairing, longer range magnetic correlations, especially of the sort one would expect near a magnetic quantum critical point, do *not* appear to be particularly favorable for superconductivity. (This final conclusion follows from a comparison of the t'/t dependence of the magnetic correlation length and the superconducting pairing in Figs. 6 and 4, respectively.)

In addition, we found that the two-leg ladder at intermediate coupling (with U of the order of the bandwidth) and close to half filling is, in many respects, surprisingly well described as a “BCS-like” superconductor, in which there is a single crossover energy scale from the “normal” to the “superconducting” state (rather than two separate scales, associated with pairing and phase coherence). This is based on the fact that the ratio of the pairing and phase coherence scales (defined in Eq. 7) is close to its weak-coupling value, which justifies the identification of the spin gap ΔE_s (or the pair binding energy ΔE_p) as the relevant energy scale for superconductivity.

Finally, there are a couple of unresolved issues and further directions we would like to highlight: 1) The extrapolation of the present results to higher dimensions is, of course, the most important open issue. The strong qualitative similarity between the present results and those obtained by exact diagonalization and CORE calculations on relatively small 2D clusters certainly encourages us to believe that the results obtained here give insight into the behavior of the higher dimensional problem. In this context, it might be useful to carry out similar calculations on 4 leg and possibly even 6 leg ladders and cylinders, although it is considerably more difficult to extend these results to such long systems as are accessible for the 2 leg ladder. 2) It is not clear exactly what aspects of the local electronic structure are essential features of an optimal inhomogeneity for superconductivity. In the present case, it is notable that pair-binding does not occur on an isolated dimer or six-site rectangle for any value of U/t , while there is pair-binding on an isolated square for $U/t < 4.6$. However, this observation does not provide an entirely satisfactory account of our findings, since the optimal pairing in the checkerboard ladder occurs for $U/t = 4 - 8t$, where the pair-binding energy of an isolated square is either small or negative.

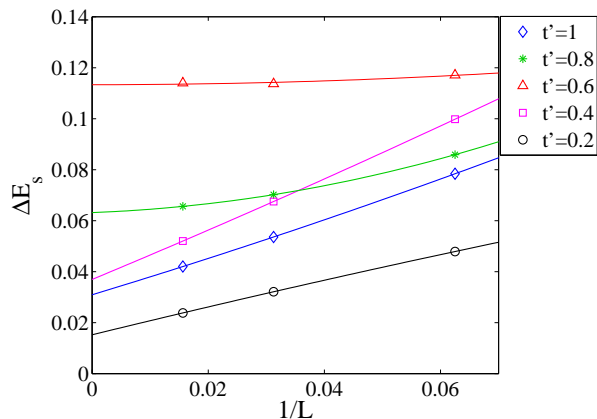


FIG. 10. Spin gap ΔE_s as a function of $1/L$ for systems of sizes $2 \times L$ where $L = 16, 32, 64$, with $n = 0.875$, $U/t = 8$, and various values of t'/t . Symbols: DMRG results, solid lines: second order polynomial fits.

ACKNOWLEDGMENTS

We thank Ehud Altman, Assa Auerbach, Malcolm Beasley, Thierry Giamarchi, Lilach Goren, Dror Orgad, Didier Poilblanc, Doug J. Scalapino, Alexei Tsvelik, and Wei-Feng Tsai for useful discussions. This research was supported by the NSF under Grants DMR-0531196 (SAK), SIMES under Grants DMR-0197960 (GK), DMR-0907500 (SRW), DMR-0705472 and DMR-0757145 (EB).

Appendix A: Extrapolation to the thermodynamic limit

The physical quantities reported in this paper are mostly extrapolated to the thermodynamic ($L \rightarrow \infty$) limit. This is done by calculating the corresponding quantity for various system sizes (typically we have used $L = 16, 32$ and 64 rungs) and then extrapolating to the limit $1/L \rightarrow 0$. As an example of this procedure, we present the spin gap ΔE_s for $n = 0.875$, $U = 8t$ and various values of t'/t , as a function of $1/L$, in Fig. 10. We use a second order polynomial in $1/L$ to fit the data and extrapolate, which in most cases fits the finite size data well.

Overall, the extrapolation to the thermodynamic limit gives a correction of up to about 30% to the measured values, making it the largest source of error in our calculations. (DMRG truncation errors are typically smaller than the symbol sizes in Fig. 10). Interestingly, the amount of extrapolation needed is smallest at values of t'/t which correspond to the maximum spin gap. We found that this behavior repeats itself for other values of n and U/t .

Appendix B: Inter-chain mean-field theory

In this Appendix, we describe the inter-chain mean-field treatment of the quasi one dimensional system described in Sec. VI. This procedure is quite standard^{23–25}. We consider an array of plaquette ladders, modelled by Luther–Emery liquids. For simplicity, we will assume that each ladder is a single component system with a spin gap ΔE_s . (The extension to the case of a two-component system is straightforward, and the result is qualitatively the same.) The ladders are coupled by an inter-chain hopping term of the form:

$$H_{\perp} = -t'' \sum_{\sigma, P=\pm} \sum_n \int dx \psi_{P\sigma}^{\dagger}(x, n) \psi_{P\sigma}(x, n+1), \quad (\text{B1})$$

where $\psi_{P\sigma}^{\dagger}(x, n)$ ($P = \pm$) creates a right or left moving electron with spin $\sigma = \uparrow, \downarrow$ at position x in chain n . Next, we integrate out degrees of freedom of lengthscales smaller than the spin correlation length $\xi_s \sim \frac{v_s}{\Delta E_s}$. Over such lengthscales, the system is essentially gapless and can be treated as a Luttinger liquid. To second order in t'' , the following effective inter-chain action is generated:

$$S_{\perp}^{\text{eff}} = (t'')^2 \sum_{\sigma\sigma', n} \int dx d\tau \int dx' d\tau' \langle \mathcal{T} \psi_{+\sigma}^{\dagger}(x, \tau, n) \psi_{+\sigma}(x, \tau, n+1) \psi_{-\sigma'}^{\dagger}(x', \tau', n) \psi_{-\sigma'}(x', \tau', n+1) \rangle_{0, >}, \quad (\text{B2})$$

where $\langle \dots \rangle_{0, >}$ denotes averaging over the “fast” (short-wavelength) degrees of freedom [using the decoupled ($t'' = 0$) action], and \mathcal{T} denotes time ordering. Since we are essentially performing a “coarse graining” step, increasing the cutoff of the theory from the lattice constant a to ξ_s , the region of integration in Eq. B2 is $\sqrt{(x-x')^2 + v_s^2(\tau-\tau')^2} < \xi_s$. In order to evaluate the integrand, we write the fermionic fields in bosonized form: $\psi_{P\sigma} \sim e^{i\sqrt{\pi}(\theta_{\sigma} + P\varphi_{\sigma})}$, where φ_{σ} and θ_{σ} are dual bosonic fields which satisfy $[\varphi_{\sigma}(x), \partial_x \theta_{\sigma'}(x')] = i\delta_{\sigma\sigma'} \delta(x-x')$. As usual, we introduce also charge and spin fields defined as $\varphi_{c,s} = (\varphi_{\uparrow} \pm \varphi_{\downarrow})/\sqrt{2}$, and similarly $\theta_{c,s} = (\theta_{\uparrow} \pm \theta_{\downarrow})/\sqrt{2}$. We define the fermionic Green’s function $\mathcal{G}(x, \tau) = \langle \mathcal{T} \psi_{+, \uparrow}(x, \tau, n) \psi_{-, \downarrow}(0, 0, n) \rangle_{0, >}$. Expressing $\mathcal{G}(x, \tau)$ in terms of the bosonic fields,

$$\mathcal{G}(x, \tau) \sim \left\langle e^{i\sqrt{2\pi} \left[\frac{\theta_c + \theta'_c}{2} + \frac{\theta_s - \theta'_s}{2} + \frac{\varphi_c - \varphi'_c}{2} + \frac{\varphi_s + \varphi'_s}{2} \right]} \right\rangle_{0, >} \sim \left| \frac{a^2}{x^2 + (v_c\tau)^2} \right|^{\frac{1}{8K_c}} \left| \frac{a^2}{x^2 + (v_c\tau)^2} \right|^{\frac{K_c}{8}} \left| \frac{a^2}{x^2 + (v_s\tau)^2} \right|^{\frac{1}{4}} e^{i\sqrt{2\pi}[\bar{\theta}_c + \bar{\varphi}_s]}, \quad (\text{B3})$$

where we have used the shorthand notation $\theta_c \equiv \theta_c(x, \tau)$, $\theta'_c \equiv \theta_c(x', \tau')$, $\bar{\theta}_c \equiv \theta_c(x/2, \tau/2)$, and similarly for θ_s , φ_c and φ_s . Plugging $\mathcal{G}(x, \tau)$ into Eq. B2 and performing the integral, we get that the following inter-chain Josephson

coupling term:

$$H_{\perp}^{\text{eff}} = -J_{\perp} \sum_n \int dx \Phi(x, n) \Phi^{\dagger}(x, n+1) + \text{H.c.}, \quad (\text{B4})$$

where $\Phi(x, n) = \psi_{R\uparrow}\psi_{L\downarrow} - \psi_{R\downarrow}\psi_{L\uparrow} \sim e^{i\sqrt{2\pi}\theta_c} \cos\sqrt{2\pi}\varphi_s$ and

$$J_{\perp} \sim K \left(\sqrt{1 - \left(\frac{v_s}{v_c}\right)^2} \right) \left(\frac{at''}{v_c} \right)^2 \frac{v_c}{a}. \quad (\text{B5})$$

Here, $K(\alpha) = \int_0^{\pi/2} d\lambda / \sqrt{1 - \alpha^2 \sin^2 \lambda}$ is a complete elliptic integral of the first kind. Eq. B5 contains a K_c -dependent prefactor, which we omit.

The mean-field equation for T_c is

$$zJ_{\perp}\chi(T_c) = 1, \quad (\text{B6})$$

where $\chi(T)$ is the superconducting susceptibility of a single chain, and z is the number of nearest-neighbor chains (*e.g.*, for a two dimensional array of checkerboard ladders, $z = 2$). Inserting Eqs. 2,B5 in the mean-field equation (B6), and using the fact that for the checkerboard Hubbard ladder $K_c \approx 1$ over a wide range of parameters, we obtain Eq. 15 for T_c .

-
- ¹ S. Kivelson and E. Fradkin, “Treatise of High Temperature Superconductivity”, J. R. Schrieffer and J. Brooks, editors, chapter 15 (Springer) (2007).
- ² S. R. White, Phys. Rev. Lett. **69** (1992).
- ³ R. Noack, S. White, and D. Scalapino, Physica C **270**, 281 (1992).
- ⁴ R. M. Noack, N. Bulut, D. J. Scalapino, and M. G. Zacher, Phys. Rev. B **56**, 7162 (1997).
- ⁵ W.-F. Tsai, H. Yao, A. Lauchli, and S. Kivelson, Phys. Rev. B **77**, 214502 (2008).
- ⁶ T. A. Maier, M. Jarrell, and D. J. Scalapino, Phys. Rev. B **74**, 094513 (2006).
- ⁷ S. R. White and D. J. Scalapino, Phys. Rev. B **79**, 220504(R) (2009).
- ⁸ T. Maier, G. Alvarez, M. Summers, and T. Schulthess, Phys. Rev. Lett. **104**, 247001 (2010).
- ⁹ S. Baruch and D. Orgad, arXiv:1005.0978 (2010).
- ¹⁰ E. Altman and A. Auerbach, Phys. Rev. B **65**, 104508 (2002).
- ¹¹ L. Balents and M. P. A. Fisher, Phys. Rev. B **53**, 12133 (1996).
- ¹² H. J. Schulz, Phys. Rev. B **53**, 2959(R) (1996).
- ¹³ D. Poilblanc, O. Chiappa, C. J. Riera, S. R. White, and D. J. Scalapino, Phys. Rev. B **62**, 14633(R) (2000).
- ¹⁴ V. J. Emery and S. A. Kivelson, Nature **374**, 434 (1995).
- ¹⁵ S. R. White, I. Affleck, and D. J. Scalapino, Phys. Rev. B **65**, 165122 (2002).
- ¹⁶ M.-S. Chang and I. Affleck, Phys. Rev. B **76**, 054521 (2007).
- ¹⁷ J. Bonca, J. E. Gubernatis, M. Guerrero, E. Jeckelmann, and S. R. White, Phys. Rev. B **61**, 3251 (1997).
- ¹⁸ S. R. White and A. L. Chernyshev, Phys. Rev. Lett. **99**, 127004 (2007).
- ¹⁹ D. Poilblanc, E. Orignac, S. White, and S. Capponi, Phys. Rev. B **69**, 220406 (2004).
- ²⁰ H. J. Schulz, Phys. Rev. B **59**, 2471(R) (1999).
- ²¹ J. Riera, D. Poilblanc, and E. Dagotto, Eur. Phys. J. B **71**, 53 (1999).
- ²² H. Yao, W.-F. Tsai, and S. Kivelson, Phys. Rev. B **76**, 161104(R) (2007).
- ²³ E. Orignac and T. Giamarchi, Phys. Rev. B **56**, 7167 (1997).
- ²⁴ T. Giamarchi and A. M. Tsvelik, Phys. Rev. B **59**, 11398 (1999).
- ²⁵ E. W. Carlson, D. Orgad, S. A. Kivelson, and V. J. Emery, Phys. Rev. B **62**, 3422 (2000).